Lawrence Berkeley National Laboratory

Title
The Influence of Residual Contamination on the Structure and Properties of Metal/GaAs Interfaces

Permalink
https://escholarship.org/uc/item/8v12j40x

Author
Liliental-Weber, Z.

Publication Date
1989

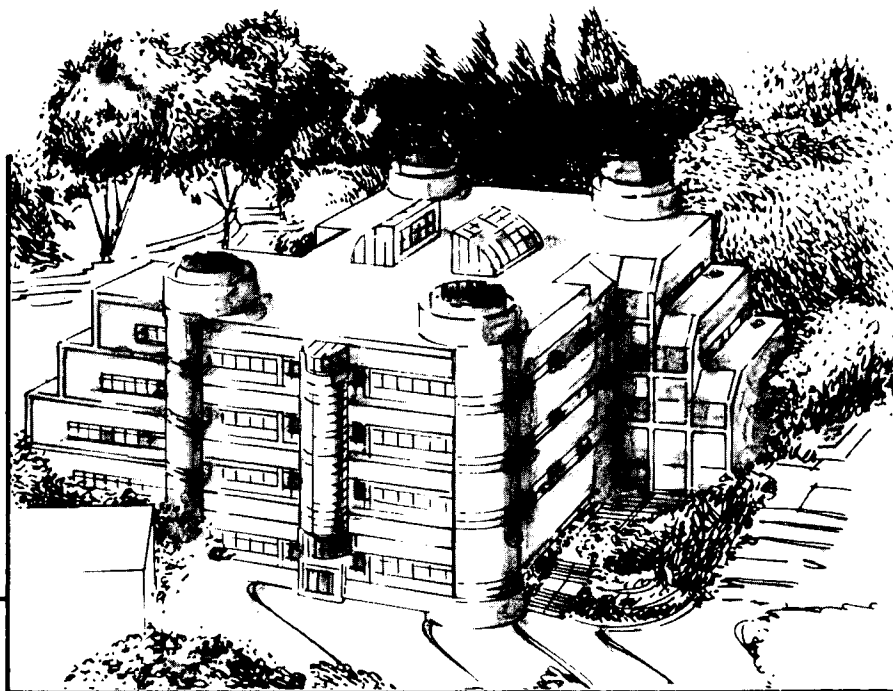**Center for Advanced Materials**

CAM

Presented at the Workshop of the International School
of Materials Science and Technology, Erice, Italy,
November 2–7, 1988, and to be published in the Proceedings

The Influence of Residual Contamination on the Structure and Properties of Metal/GaAs Interfaces

Z. Liliental-Weber

October 1988

Materials and Chemical Sciences Division

Lawrence Berkeley Laboratory • University of California

ONE CYCLOTRON ROAD, BERKELEY, CA 94720 • (415) 486-4755

DISCLAIMER

THE INFLUENCE OF RESIDUAL CONTAMINATION ON THE STRUCTURE
AND PROPERTIES OF METAL/GaAs INTERFACES

Zuzanna Liliental-Weber

Center for Advanced Materials
Materials and Chemical Sciences Division
Lawrence Berkeley Laboratory
1 Cyclotron Rd., Berkeley, CA 94720

THE INFLUENCE OF RESIDUAL CONTAMINATION ON THE STRUCTURE AND PROPERTIES OF METAL/GaAs INTERFACES

Zuzanna Liliental-Weber

Center for Advanced Materials
Lawrence Berkeley Laboratory
1 Cyclotron Rd., Berkeley, CA 94720

INTRODUCTION

Reliable and reproducible metal contacts to semiconductors are necessary if electronic devices are to function properly. Two types of contacts are required to make these devices work properly: (1) ohmic contacts, and (2) rectifying gate contacts, which in some applications must survive annealing at 800°C or higher to activate implanted dopants.

Despite the wide spread use of rectifying contacts to GaAs, two important issues remain to be resolved. One -- the basic mechanism responsible for the observed Schottky barrier heights (which is still being debated) and the second -- reproducibility and stability of electrical performance during annealing and aging.

Most experimental data agree that the barrier heights for all metals measured on GaAs fall within a few tenths of an eV in the midgap region, indicating strong Fermi level pinning mechanism at metal/GaAs interfaces. The measurements of barrier heights for many metals deposited in situ on ultrahigh-vacuum- (UHV) cleaved GaAs, as determined by Newman[1] using I-V and C-V characteristics, seem to be very consistent. They show the same ideality factor n = 1.05 independent of the reactivity of the particular metal. The lowest barrier height found on n-GaAs was for Cr (Φ_b = 0.67 eV), and the highest was for Au (Φ_b = 0.92 eV). To explain these results which are still controversial several models have been proposed.[2] In some of them the Fermi level pinning was ascribed to the inherent properties of ideal metal/GaAs interfaces (metal-induced gap states[3,4]), in others to native defects[5] which are formed upon metal deposition due to the energy which was released during metal solidification or to work-function differences between GaAs and microscopic interfacial inclusions of arsenic, metal arsenides, or impurities (the Effective Work Function model[6]). Part of our work is directed towards contributing to this fundamental problem[7-11], however in this chapter we will concentrate on our contribution to the second issue. We will show, that surface contamination is indeed a major cause for thermal and electrical instability connected with degradation of the metal/semiconductor interfaces.

Our approach was to compare the structure, electrical properties and stability of electrical properties of "ideal" contacts deposited in-situ in UHV on cleaved GaAs (110) with contacts deposited on air-exposed GaAs (110) and in some cases with technologically prepared GaAs (100) contacts. We will describe in detail our results for four different systems: Au, Ag, Al and Cr on GaAs.

Experimental Procedure

To remove any unnecessary variables (e.g., impurities on the GaAs surface), the diodes used in this study were produced on clean GaAs surfaces formed by cleaving in an ultrahigh vacuum (UHV) with the metal deposited in situ.[12] Bulk n-GaAs bars (Si doped) were placed in an UHV chamber that was baked out to obtain a vacuum of $\sim 2 \times 10^{-10}$ torr. The bars were cleaved along their {110} planes. Metals were then deposited in situ using a resistance-type evaporator without breaking vacuum or additional heating. (During deposition the vacuum was kept $< 4 \times 10^{-10}$ torr.) In order to observe the influence of contamination on the properties of the electrical and structural contacts, a second batch of metal diodes was deposited on samples cleaved in air in the same vacuum chamber. In order to assure that the air-exposed surfaces were not subjected to any unnecessary heat before metalization, a chamber bakeout was not performed. For the diodes produced on the air-exposed surfaces, the pressure during the metal deposition was approximately 10^{-7} torr. The metal thickness for these two kind of diodes was ~ 100 nm. These two kinds of samples were annealed for 10 min at 405°C in a N_2 atmosphere.

In order to compare these diodes with diodes formed using typical commercial GaAs processing technology, a third batch of samples was prepared by deposition of Au layers on chemically cleaned samples. Au was chosen as the most frequently used metalization element. Electron-beam evaporation was used in the contact-fabrication process. The annealing was performed in a 95% Ar – 5% H_2 environment at the same time and temperature as for the first two batches of samples.

The structure and electrical properties of all contacts on GaAs were investigated by analytical and high-resolution transmission electron microscopy (TEM), combined with electrical characterization.

Electron microscopy was performed at LBL's National Center for Electron Microscopy in Berkeley using the JEOL JEM 200CX electron microscope equipped with a high-resolution pole piece (~ 0.25 nm point-to-point resolution) and the 1-MeV Atomic Resolution Microscope (ARM), which has a point-to-point resolution of ~ 0.16 nm.

Au Contacts[7-14]

The as-deposited Au layer was found to be polycrystalline in all three cases, with grain diameters in the 10-50 nm range. The largest grain size was found in UHV-deposited Au samples. Some of these grains were twinned along (111) planes. Such unannealed Au layers observed in cross sections show atomically flat interfaces with GaAs. Some of these grains, particularly in UHV-cleaved samples, were in the (211) or (011) orientation parallel to the (011) GaAs substrate orientation, but generally the grains were randomly oriented, resulting in diffraction patterns with textured rings.

Significant differences between these samples occur after annealing in N_2 at 405°C for 10 min (Fig. 1). For the UHV-cleaved samples, the interface remains flat and abrupt despite the annealing process
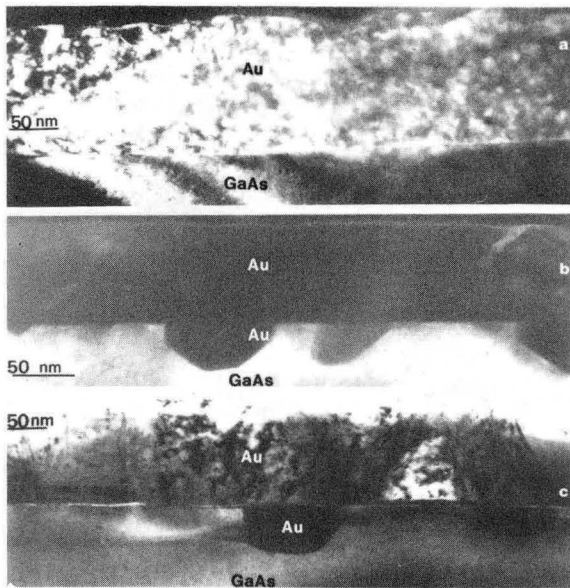
Fig.1. Cross sections of annealed Au/GaAs interfaces. (a) Au deposited _in situ_ on (b) Au deposited UHV-cleaved GaAs, on GaAs cleaved in air, (c) Au deposited on chemically clean GaAs. XBB 862-1034

[Fig. 1(a)]. The entire Au layer was almost monocrystalline, with the smallest grain size ~ 500 nm. Most of the grains were elongated along $[011]_{GaAs}$. Their orientation relationship towards the substrate was $(211)_{Au}$ slightly tilted from $(011)_{GaAs}$ e.g. $(522)_{Au}$ being parallel to $(011)_{GaAs}$. A perfect match between the substrate and the Au layer is expected for each fifth $\{200\}_{GaAs}$ plane with each sixth $\{111\}_{Au}$ plane. In many areas triangular features elongated along $[011]_{GaAs}$ were observed. These triangular features are just cross sections of prism-shaped features observed in plan-view samples (Fig. 2). These features probably voids were formed in the Au layer directly adjacent to the GaAs substrate [Fig. 2(a)]. High-magnification images using the ARM showed that these areas consisted of amorphous material with embedded gold particles.

The same annealing treatment for the Au samples deposited on GaAs cleaved in air resulted in the formation of metallic protrusions at the interface [Fig. 1(b)]. Many small grains, highly twinned and dislocated with irregular shapes, were observed in a plan view of annealed air exposed samples. The larger grains had two different shapes, triangular and rectangular.

In cross sections two different shapes of protrusions were found extending into the GaAs [(Fig. 1(b)]: (1) triangular protrusions whose sides are delineated by GaAs $\{111\}$ planes, and (2) multifaceted protrusions delineated by GaAs $\{111\}$, $\{110\}$, and $\{100\}$ planes. These two different protrusion shapes are probably related to the two different grain shapes visible in plan-view samples. Such protrusions were observed in the past for annealed Au-Ni-Ge contacts[15,16] and Au contacts,[17] and it was concluded that elevated temperatures are a sufficient condition for their formation. It is interesting to note that those protrusions were elongated along $[011]_{GaAs}$ [Fig. 2d], as were void-like features in the samples deposited in UHV and subsequently annealed [Figs. 2b and 2c]. Because the protrusions and void-like features are elongated in the same crystallographic direction, they can be easily misinterpreted by SEM type of studies. For many grains in air-exposed samples the $(011)_{Au} \| (011)_{GaAs}$ relationship was observed, but for some other grains $(\bar{4}11)_{Au} \| (011)_{GaAs}$ was found as well. Details about the relationship will be discussed in the next chapter.

Even more complicated interfaces were observed in annealed Au/GaAs samples formed on chemically prepared GaAs surfaces. The gold layer was separated from the GaAs substrate by a thin oxide band. Oxygen was
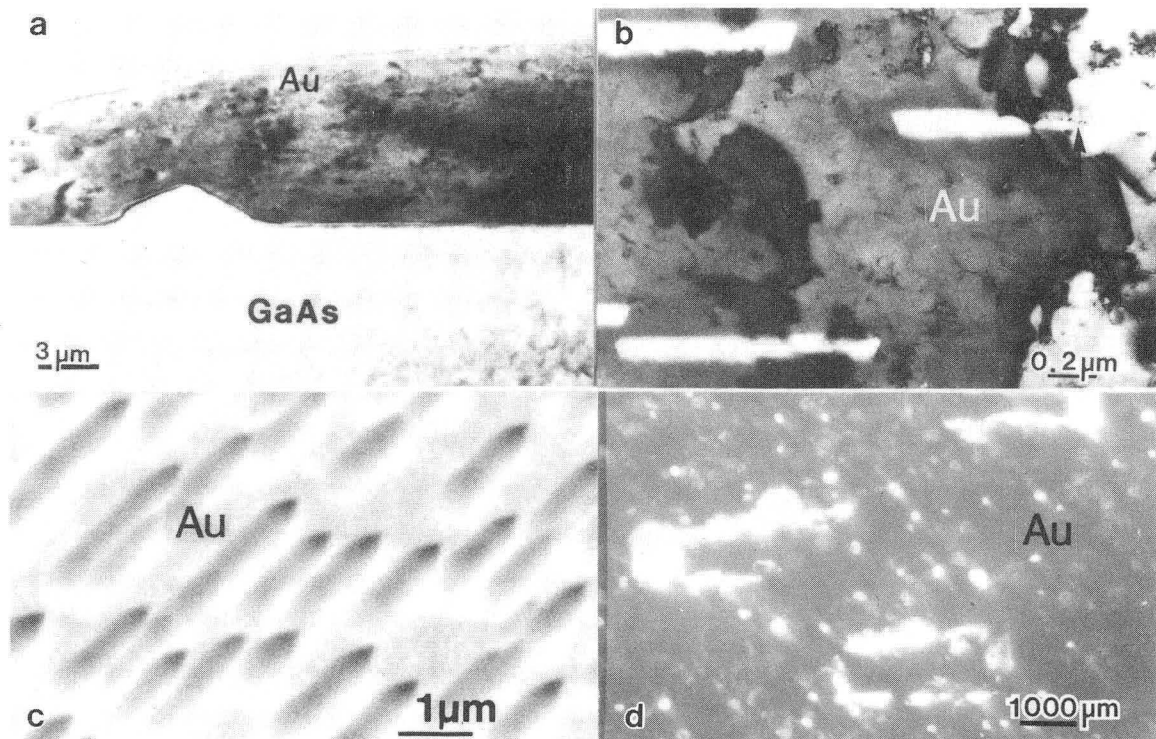
3

Fig. 2.(a)TEM micrograph of cross section of Au/GaAs interface from the sample prepared *in situ* in UHV on cleaved GaAs after annealing in N_2 at 405°C for 10 min. The image was taken in the [011] zone axis. Note void-like triangular features formed in Au adjacent to the GaAs substrate. A high-magnification image of these triangular areas shows embedded Au particles inside the triangular areas. The same triangular features elongated along [011] are shown in plan view by TEM (b) and by SEM (c); (d) Plan-view image of Au sample prepared by deposition on an air-exposed cleaved GaAs surface annealed under the same conditions. Note the long grains elongated along [011]. These grains are the protrusions embedded in the GaAs substrate shown in Fig. 1(b). XBB 880-10080

detected on the interface by energy-dispersive x-ray spectroscopy (EDX) in chemically prepared samples and in the samples cleaved in air.[14] Oxygen was not detected in samples where Au was deposited *in situ* on the UHV-cleaved surface. In many areas, the interface was found to be very flat and abrupt [Fig. 1(c)]. However, islands of gold with a wide range of shapes were found below the oxide layer as well. These islands were epitaxially regrown, with a much smaller defect density than in the layer above the oxide. The observation of separated islands below the oxide layer would suggest that Au has diffused through already exiting pinholes in the oxide. The orientation relationship for those grains was similar as for air-exposed samples, e.g. $(011)_{Au} \| (011)_{GaAs}$.

The Au layer above the oxide layer has many defects, and the grain size is much smaller than the annealed Au deposited in UHV.

These observations show that GaAs is very sensitive to oxidation and that the morphology of the interface is strongly influenced by the surface preparation prior to Au deposition. This demonstrates that the formation of protrusions is not the result of annealing at elevated temperatures alone but is clearly affected by the semiconductor surface-preparation technique prior to metal deposition.

4

As determined from I-V characteristics, there was not a large difference in barrier height for the Au diodes deposited in situ on UHV-cleaved GaAs samples (0.92 eV) and deposited on the samples cleaved in air (0.83 eV). After annealing, the barrier height decreases to 0.72 eV for both kinds of samples. A very important observation[18,19] is that those samples that were air exposed before Au deposition were found to age with time and/or exposure to electrical measurements where large bias voltages were used, whereas UHV-cleaved samples were stable. This observation is a very important consideration for the reliability of practical devices built on oxidized surfaces.

Ag Contacts[18-22]

Two kinds of Schottky diodes, similar to the first two kinds of Au diodes, were prepared for Ag: deposited on clean, UHV-cleaved (110) GaAs, and deposited on air-exposed cleaved (110) substrates.

Significant differences in the structures of the two kinds of contacts were observed. The metal/substrate interface was flat in both cases [Figs. 3(a) and 3(c)] for as-deposited samples; however, in the air-exposed samples an oxide layer ~ 40 Å thick was present on the GaAs surface. This oxide layer varied in thickness along the interface. The air-exposed diodes contained a higher density of twins and much smaller Ag grains in the metal layer than did the samples deposited in UHV conditions.

As in Au case, a difference in interface morphology was observed for these two kinds of samples after annealing. The interface remained flat for the UHV samples, and high-resolution electron microscopy showed that that $\{111\}_{Ag}$ planes were rotated slightly toward the $\{200\}_{GaAs}$ planes [Fig. 3(b)]. Large protrusions were formed at the interface of the air-exposed samples [Fig. 3(d)]. The faceted Ag protrusions grew into the GaAs. One of the facet planes of such a protrusion was always parallel to $\{111\}_{GaAs}$ and the other plane varied, but in many cases the other facet plane was parallel to $\{122\}_{GaAs}$.[21] When plan-view samples were prepared by ion-milling from the substrate side with partial Ag removal by short ion-milling from the metal side, it was clear that all these protrusions were embedded into the GaAs substrate, as was expected from cross-section samples, and that these protrusions were elongated along $[011]_{GaAs}$.[21] Also, as was the case for the annealed Au samples deposited on the air-exposed substrate, the orientation relationship for air-exposed samples was $[011]_{GaAs} \parallel [011]_{Ag}$ with $(011)_{GaAs} \parallel (011)_{Ag}$.

After annealing, voids formed at the metal/GaAs interface in many areas, and a large portion of the Ag layer peeled off. These void formations were observed in as-deposited air-exposed samples, but adhesion decreased after annealing. Occasionally adhesion problems occurred in UHV-deposited samples as well, but the problems were not so drastic as they were with the air-exposed samples after annealing. Many more problems occurred in those samples that remained in air longer before metal deposition and subsequent annealing.

The Schottky barrier height measured from I-V curves was 0.96 eV for as-deposited air-exposed samples, higher by 70 meV than that of UHV-cleaved diodes.[19] After annealing, a slight increase in barrier height (0.91 eV) was observed for UHV-deposited samples, while a large decrease (0.79 eV) and leakage was observed for air-exposed samples (Fig. 4). The large leakage current often reported in the literature[21-23] can be correlated with the adhesion problems in those samples.
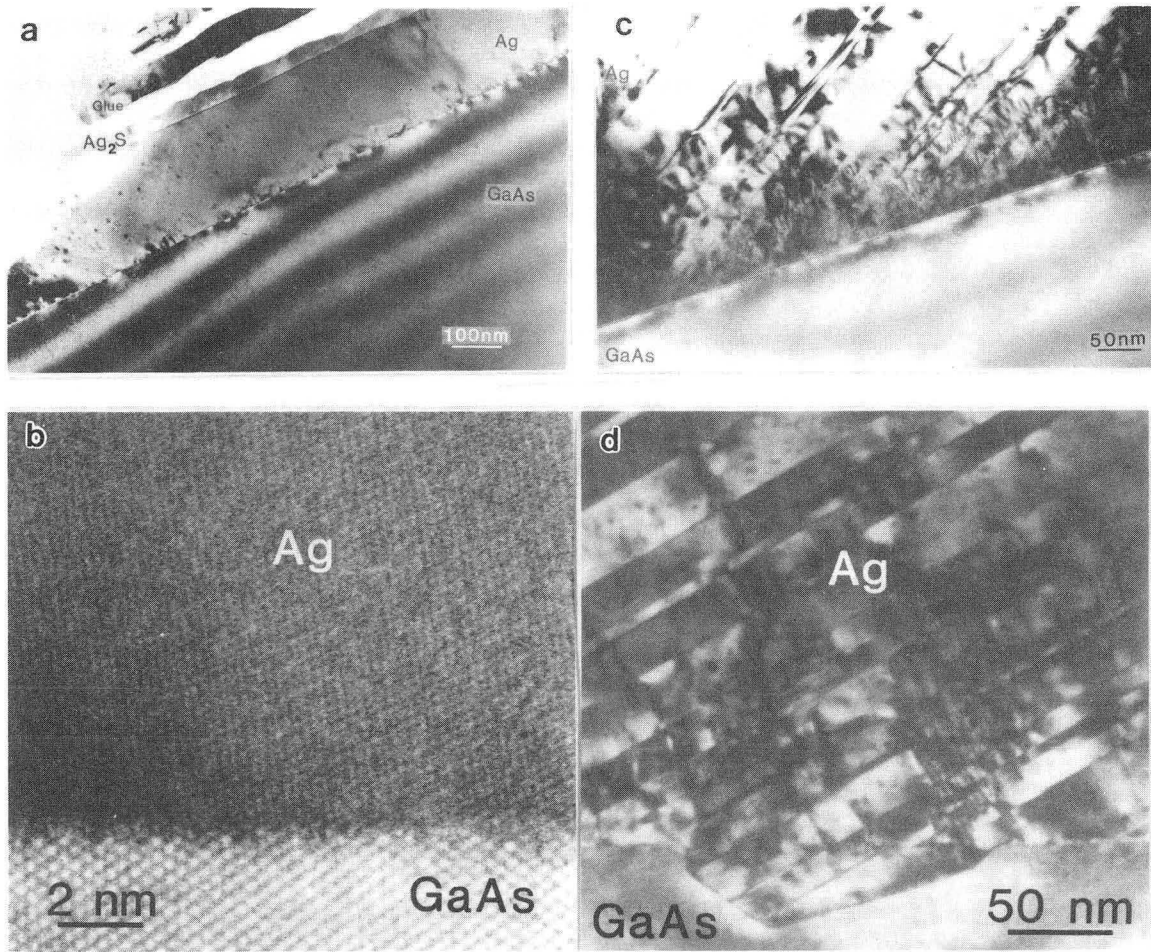
5

Fig. 3. Cross-section micrographs of Ag/GaAs interfaces. (a) Ag deposited *in situ* on UHV-cleaved (110) GaAs. Note the very large Ag grain size. (b) High-resolution image of sample prepared under the same conditions as (a) after annealing in N_2 at 405°C for 10 min. (c) Ag deposited on air-exposed cleaved (110) GaAs, showing a high density of twins and an oxide layer formed on the interface. (d) Sample (c) annealed at 405°C in N_2. Note protrusion at the interface, a twinning of the Ag layer. XBB 870-10294 top a); XBB 870-10295 top b); XBB 880-10079 c)
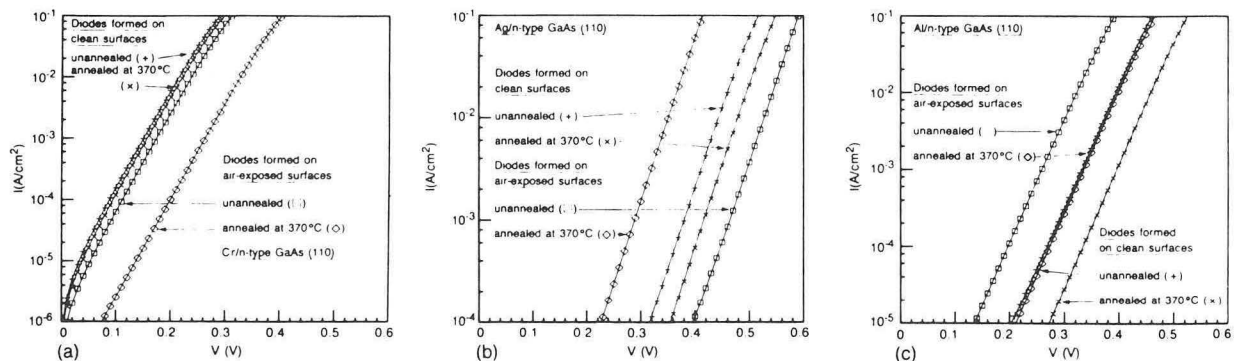

Fig. 4. Typical current-voltage (I-V) measurements for diodes a) Cr, b) Ag, c) Al formed on clean n-type GaAs (110) surfaces prepared by cleavage in UHV and on air-exposed surfaces prepared by cleavage and exposure to the atmosphere for ~ 1-2 hrs. XBL 8810-3597

6

Electrical aging was performed for as-deposited air-exposed and UHV-cleaved samples.[18-20] For UHV-cleaved Ag diodes, electrical aging was performed with current densities from $2 \times 10^{-2} A/cm^2$ (0.60 V) up to 1.4 A/cm^2 for reverse bias (-19 V). For the UHV-cleaved Ag diodes, no significant change in barrier height and ideality factor was found after electrical aging under these conditions for more than 7 hrs. By contrast, for air-exposed Ag/GaAs diodes, 50 min at $4.3 \times 10^{-5} A/cm^2$ (-14 V) was sufficient to decrease the barrier height by 20 meV. More severe conditions of $2.3 \times 10^{-3} A/cm^2$ (-17 V) for the same 50-min period decrease the barrier height by 75 meV (Fig. 5).

Electrical aging reduced the barrier-height difference between the two kinds of diodes without significantly changing the ideality factor of either kind of diode (n = 1.06-1.085). Thus electrical aging caused changes in barrier height but did not significantly deteriorate the near-ideal Schottky characteristics of the diodes. It was also observed that the changes in barrier height were not stable: the Schottky barrier height returned almost to its initial value (before current stressing) within about five days. Light or forward current accelerated this recovery effect.

Current stressing of UHV-cleaved diodes did not result in any structural changes, but the air-exposed contacts showed a significant change.[18-20] Current stressing caused a decrease in the size of the Ag grains, the formation of voids separating these grains, and poor adhesion of the metal overlayer. Local electromigration of Ag resulted in Ag accumulation in parts of the contact and thinning or void formation in other parts[20]. Electromigration of Ag in the air-exposed diodes may be the result of large local current densities due to an inhomogeneous interfacial oxide layer, which acts to block current flow over part of the area of the contact.

The observations of void formation, enhanced electromigration combined with the formation of new compounds, can explain why Ag Schottky contacts, which are known to be generally leaky, have not been applied successfully in GaAs device technology. However, this study has shown that very stable and reliable Ag contacts can be obtained if the Ag is deposited on atomically clean surfaces, such as the UHV-cleaved surfaces used for these observations.

Al Contacts[9,18,19,24]

For Al deposited on UHV-cleaved GaAs, the grain size of 100-300 nm was observed. The interface with GaAs remains flat and the Al (111) planes form a small angle with the GaAs (111) planes (Fig. 6). This angle remains constant for grains with different orientations. Upon annealing at 375°C in N$_2$ for 10 min, the interface remains flat and
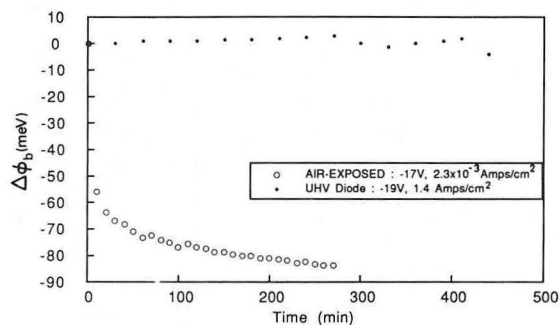

Fig. 5. Typical results of electrical aging for Ag/n-type GaAs (110) diodes formed on air-exposed and UHV-cleaved GaAs (110) surfaces. The change in barrier height is plotted as a function of the time the diodes were exposed to electrical aging. XBL 8712-5209
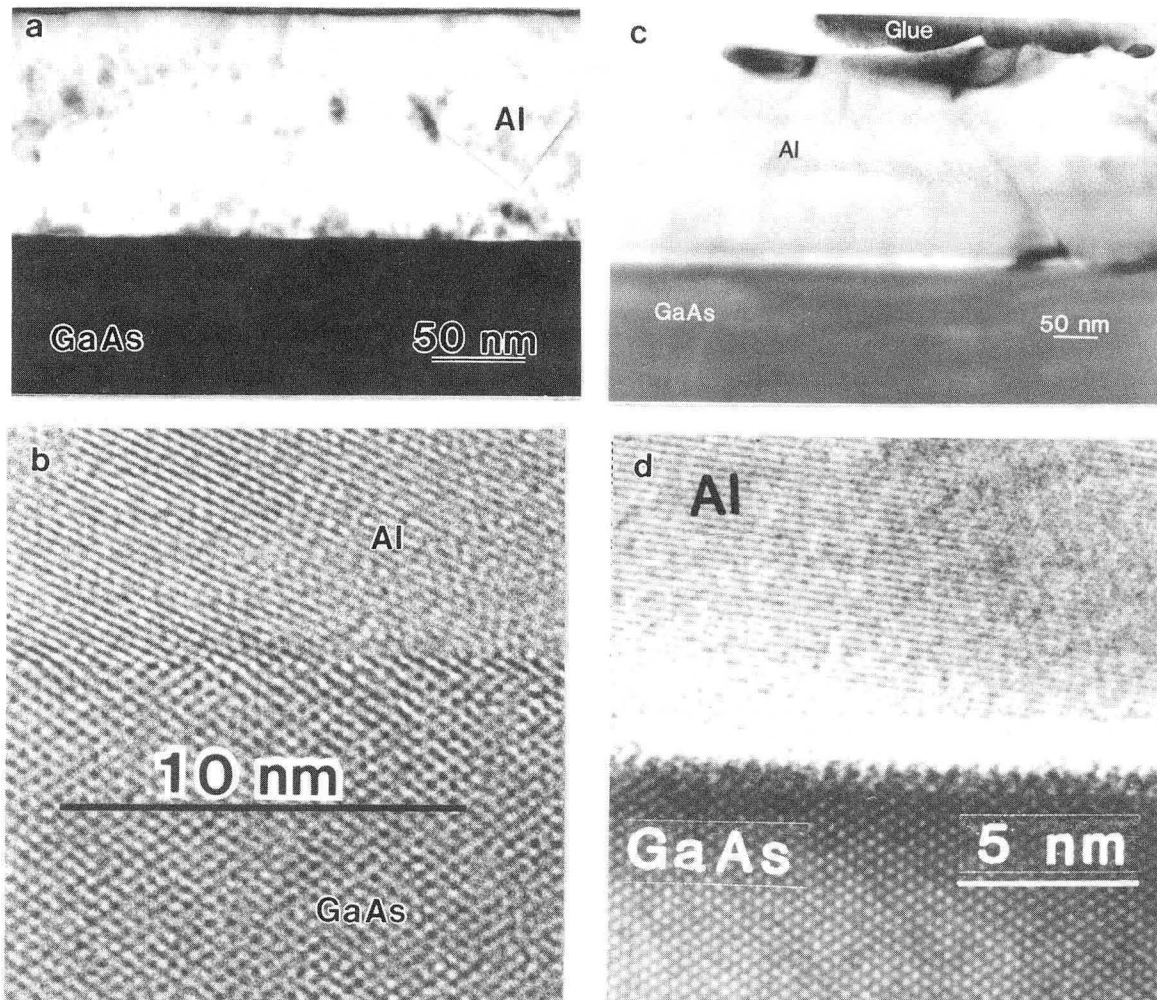
Fig. 6. TEM micrograph of cross sections of Al/GaAs interfaces (a) from the sample prepared on UHV-cleaved substrate; (b) high-resolution image of the same sample annealed at 405°C in N_2; (c) from the sample prepared on air-exposed GaAs; (d) high-resolution image of the same sample annealed under the same conditions. Note amorphous layer at the interface. XBB 8610-8793; XBB 868-6147; XBB 880-10081; XBB 880-10082

the grain size does not increase. In some areas a very thin layer (50-100 Å) of AlGaAs was formed. The formation of AlGaAs did not occur uniformly. There were large areas where this phase was not detected.[9,24] Individual grains of Al above AlGaAs or in intimate contact with GaAs did not change the orientation relationship upon annealing.

For the samples cleaved in air, the interface remained flat before and after annealing, but a significant decrease in Al grain size was observed in these samples. In some areas of the annealed air-exposed samples, a thin layer of AlGaAs was detected as well. For Al metalization, in contrast to the previously described metals (Au and Ag), no protrusions at the interface were observed for cleaved air-exposed samples after annealing. This probably can be explained by the formation of an AlGaAs phase in intimate contact with GaAs and no As outdiffusion from the systems.

In all observed cases, Al (or AlGaAs) was always found in intimate contact with the GaAs substrate. Void formation was not observed,

either in as-deposited samples or in annealed ones. Aging of these contacts did not influence the interface structure.

Al deposited _in situ_ on UHV-cleaved GaAs forms Schottky contacts with a barrier height of 0.83 eV (Fig. 4c). After _ex situ_ annealing for 10 min in N_2 atmosphere at 360°C or above, the barrier height increases to 0.90 eV.[19,25] This is in contrast to the behavior of the Au diodes, where the barrier height decreases upon annealing. For as-deposited samples cleaved in air, the barrier height was lower (0.76 eV) than for UHV-cleaved samples, but a similar increase of 70 meV was observed after annealing.[19,25] The increase of barrier height for AlGaAs upon annealing has frequently been attributed to the formation of the interfacial AlGaAs with a larger bandgap.[26,27] However, recent studies showed, that the barrier height of Al on n-GaAs (110) added up together with the barrier height of Al on p-GaAs to the GaAs bandgap.[28] The observed changes in barrier height are thus due to a downward shift of the Fermi level pinning position rather than the formation of AlGaAs. We have attributed this shift of the Fermi level pinning position to a change of stoichiometry due to the replacement of Ga by As.[9,10]

Air-exposed Al/GaAs diodes were aged at -9.7 V for more than 7 hrs with a reverse current flow of 1.3 A/cm^2. There was a very small, almost insignificant, increase of ~ 9 meV in the barrier height after electrical aging. No change in barrier height was noticed for UHV-deposited samples with the same aging parameters. This study shows that Al contacts are stable upon annealing. Strong adhesion between Al and the substrate exists for both UHV-deposited and air-exposed samples. No protrusions were found at the interfaces upon annealing.

Cr Contacts[18,19,29]

The TEM study of Cr layers deposited on clean UHV-cleaved GaAs surfaces consistently showed a columnnar structure in the Cr layer. These columns were inclined 80° to the interface, and this inclination was probably related to the deposition direction. The size of the columns was in the range of 4-12 nm. Voids up to 5 nm wide were formed between some of the columns. The void formation initiated in the Cr layer, about 10-15 nm from the interface with the GaAs [Fig. 7(a)].

High-resolution images of the interface taken in the ARM (1 MeV) in [100] and [110] projections show that the interface with GaAs was flat on an atomic scale. The individual columns were misoriented with respect to each other by a few degrees [Fig. 7(c)].

The orientation relationship between the GaAs substrate and the Cr layer was $\{100\}_{Cr} \| \{100\}_{GaAs}$ with $[011]_{Cr} \| [022]_{GaAs}$. Cr matches GaAs almost perfectly to GaAs because the Cr lattice parameter (a = 0.288 nm) is almost exactly half that of GaAs (a = 0.565 nm).

For the samples with Cr deposited on the air-exposed GaAs surface, the interfaces were flat, similar to the UHV-deposited samples. A columnar structure of the Cr overlayer was observed as well, but the columns were almost randomly oriented, with a high void density between them [Fig. 7(b)]. The size of the columns of these samples was less than 2 nm. Extra spots of chromium oxide were detected in these samples.

Annealing for 10 min in N_2 at atmospheric pressure at 370°C did not cause the formation of a new phase in either the UHV samples or the air-exposed samples.
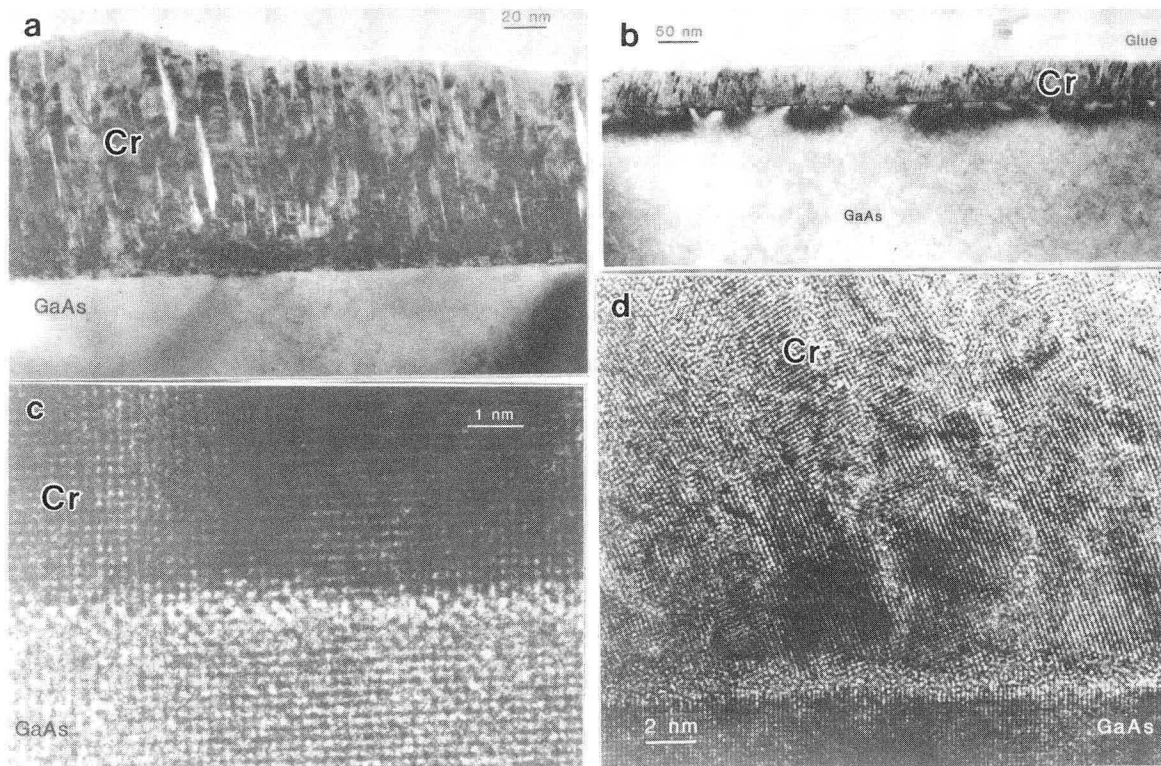
Fig. 7. TEM micrographs from Cr/GaAs interfaces: (a) low-magnification micrograph showing columnar structure of Cr with voids between columns for UHV as-deposited samples. Note that columns are almost parallel to each other and inclined ~ 80° toward the interface with GaAs; (b) low-magnification micrograph showing columnar structure of Cr with columns inclined in a different direction to the substrate for air-exposed samples; (c) high-resolution micrograph of annealed samples deposited in UHV. Note two perpendicular (110) planes in a Cr column to the left and only one set of lattice images for the planes parallel to the substrate in the second column (darker image); (d) high-resolution image of annealed air-exposed samples. Note thick oxide layer at the interface and increased buckling of lattice planes toward the top of the layer. (a) XBB 885-5787, (b) XBB 885-5284, (c) XBB 885-5288, (d) XBB 885-5283

High-resolution images from annealed UHV samples show that the structure and interface abruptness remained stable after annealing. Individual columns remained slightly misoriented to one another [Fig. 7(c)].

A high-resolution image of the air-exposed samples showed an oxide layer about 1 nm thick at the interface [Fig. 7(d)]. Voids between columns remained after annealing. Individual columns and lattice planes were found to change their inclination direction continuously with increasing layer thickness. The top of the layer consisted of small polycrystalline Cr grains.

I-V and C-V characteristics taken on both types of as-deposited diodes showed a barrier height of 0.66 eV for UHV-cleaved samples and 0.68 eV for air-exposed samples (Fig. 4). This small difference was within measurement error. It shows that an oxide layer at the interface does not influence the barrier height for as-deposited samples. Similar values (0.69 eV) were reported for UHV-cleaved samples by McLean and

10

Williams,[30] and slightly higher values (0.73 eV) were reported for Cr/GaAs (100) by Waldrop.[31]

The barrier height (0.68 eV) and ideality factor (n = 1.06) of the UHV-deposited contacts, as determined by I-V electrical measurements, did not a change upon annealing at these temperatures (see Fig. 4).

For air-exposed samples the barrier height increased (Fig. 4) from 0.68 eV to 0.76 eV after annealing. The low barrier height of Cr (0.66 eV) for as-deposited samples (compared to other metals, e.g., 0.92 eV for Au) may be associated with the accumulation of As near the interface.[7,10]

Aging of Cr diodes at -19 V for more than 6 hrs with a reverse current flow of 3 A/cm^2 did not change the barrier height by more than 6 meV (within experimental error) for either UHV-cleaved samples or air-exposed ones.

Orientation Relationship in Metal/GaAs Interfaces[9]

The orientation relationship between the metals investigated (Au, Ag, Al, and Cr) for as-deposited samples was almost random for all samples. When the metals were deposited in situ on UHV-cleaved samples, the metal grains were always larger than those of the metals deposited on the air-exposed GaAs substrate.

The difference in orientation relationship between differently prepared samples occurred after annealing. These differences are shown for Au in Table 1 and described in detail in Ref. 9.

Table 1. Orientation relationship between Au and GaAs.

Crystallographic axis	x	y	z
GaAs	011	100	0$\bar{1}$1
Type I	011	100	0$\bar{1}$1
Type IIa	$\bar{4}$11	122	0$\bar{1}$1
Type IIb	$\bar{4}$11	0$\bar{1}$1	$\overline{1}$22
Type III	$\bar{5}$22	455	0$\bar{1}$1

Type I orientation relationships were observed for all air-exposed samples (Au, Ag, Cr) except Al. This type of orientation relationship was explained for Au by Yoshiie and Bauer[32] as the epitaxial relationship to the newly formed Au-Ga phase, e.g., (01$\bar{1}$)$_{GaAs}$||(1$\bar{1}$0)$_{AuGa}$|| (01$\bar{1}$)$_{Au}$ with [01$\bar{1}$]$_{GaAs}$|| [001]$_{AuGa}$ || [01$\bar{1}$]$_{Au}$. However, formation of an Au-Ga phase is not necessary to fulfill the minimum mismatch on the interface. The mechanism is probably more general. Our data show that the Au orientation relationship for cleaved (110) GaAs surfaces depends on both the environment in which the GaAs surface was prepared before annealing and the annealing conditions, and not necessarily on the Au-Ga phases formed. The type I orientation relationship exists in annealed Au even when an Au-Ga phase is not formed, but it is characteristic for annealed Au deposited on air-exposed GaAs and exists for other metals like Ag, where this phase is not formed. A possible explanation for this behavior is that the γ-Ga$_2$O$_3$ grows epitaxially[33,34] as a

type I orientation: $(011)_{Ga_2O_3} \parallel (011)_{GaAs}$ with $[100]_{Ga_2O_3} \parallel [100]_{GaAs}$. This oxide provides an excellent lattice match to Au: d_{400} $(Ga_2O_3) = 0.205$ nm, as compared with d_{200} (Au) $= 0.203$ nm (with similar d values for Ag and Cr) and d_{044} $(Ga_2O_3) = 0.145$ nm, with d_{022} (Au) $= 0.149$ nm. This observation would suggest that as soon as GaAs is exposed to air, epitaxial γ-Ga_2O_3 is formed, and the deposited metal epitaxially relates to the oxide already existing at the interface.

The oxide on GaAs is not a continuous layer. In the areas where the oxide is not present, twinning takes place, giving a better match at the interface, leading to a type IIa orientation relationship. A type IIb orientation was observed in most cases for Au deposited on UHV-cleaved GaAs with in situ postannealing.

The orientation relationship in UHV-deposited Au samples annealed ex situ in N_2 (405°C, 10 min, as done for air-exposed samples) was completely different and was described as type III. This type of orientation relationship was observed not only in Au/GaAs samples but also in Al/GaAs and Ag/GaAs samples. A small rotation angle ($\sim 10°$) between $(111)_{Au,Ag,Al}$ planes and $(111)_{GaAs}$ planes was characteristic for all three metals (they have similar lattice parameters) deposited in situ on UHV-cleaved GaAs and annealed in N_2. This behavior was explained by As accumulation at the interface.[9,10] The metal probably tries to accommodate to the accumulated As or to the As plane in the GaAs substrate. This discussion shows, that the macroscopic orientation relationship of metal grains on GaAs is very sensitive to interfacial contamination. Comparing of the crystallographic orientation relationships of metal grains on GaAs (110) revealed distinct differences between UHV-deposited and air-exposed samples. In fact, the observation of the orientation relationship after annealing for metals with similar lattice parameters can be used as an additional tool in recognizing how clean the GaAs surface was before metal deposition. All metals deposited on air-exposed substrates follow the orientation relationship of the oxide present on the semiconductor surface.

CONCLUSIONS

This study shows that interface morphology, orientation relationship, and formation of new phases strongly depend on the surface preparation of GaAs before metal deposition and/or on the annealing environment. The metals investigated (Au, Ag, and Al, with lattice parameters close to each other) deposited in situ on a UHV-cleaved GaAs surface show very similar relationships with GaAs upon annealing. This relationship changes when GaAs is exposed to air before metal deposition. All metals investigated, when deposited on a UHV-cleaved GaAs substrate, are stable upon annealing. The interface between metal and GaAs remains abrupt upon annealing. In the case of Cr almost perfect matching to GaAs was observed for UHV deposited samples, but random orientation for air-exposed samples.

This study shows that impurities at the semiconductor surface can affect the stability of the barrier height of Schottky contacts. These changes in barrier height depend on the metal used, and on the intensity and direction of the potential and current during the electrical aging. The dramatic example of Ag contacts and their change upon current stressing only for air-exposed samples confirms the importance of surface preparation before metalization.

A great part of frequently observed problems with reproducibility and stability of Schottky barrier heights on GaAs can be ascribed to

insuffient cleaning of water surfaces before metal deposition. Comparison of the results of current processing with UHV-prepared samples allows in a unique way to define the goals available for non-contamination technology.

REFERENCES

1. N. Newman, M. Van Schilfgaarde, T. Kendelewicz, M. D. Williams, and W. Spicer, Phys. Rev. B 33, 1146 (1986).
2. J. Vac. Sci. Technol. B, Vol. 5, No. 4, Jul/Aug 1987.
3. V. Heine, Phys. Rev. A 138, 1689 (1965).
4. J. Tersoff, Phys. Rev. Lett. 52 465 (1984).
5. W. E. Spicer, Z. Liliental-Weber, E. Weber, N. Newman, T. Kendelewicz, R. Cao, C. McCants, P. Mahowald, K. Miyano, and I. Lindau, J. Vac. Sci. Technol. B6, 1245 (1988).
6. J. L. Freeouf and J. M. Woodall, Appl. Phys. Lett. 39, 727 (1981).
7. Z. Liliental-Weber, N. Newman, W. E. Spicer, R. Gronsky, J. Washburn, and E. R. Weber, in Thin Films--Interfaces and Phenomena, edited by R. J. Nemanich, P. S. Ho, and S. S. Lau (Materials Research Society, Pittsburgh, 1986), Vol. 54, p. 415.
8. Z. Liliental-Weber, R. Gronsky, J. Washburn, N. Newman, W. E. Spicer, and E. R. Weber, J. Vac. Sci. Technol. B4, 912 (1986).
9. Z. Liliental-Weber, J. Vac. Sci. Technol. B5, 1007 (1987).
10. Z. Liliental-Weber, E. R. Weber, N. Newman, W. E. Spicer, R. Gronsky and J. Washburn, "Defects in Semiconductor" in Material Science Forum Vol. 10-12, 1986 p. 1223 edit. H. J. von Bardelebon, Trans. Tech. Publ. Ltd., Switzerland.
11. W. E. Spicer, Z. Liliental-Weber, E. R. Weber, N. Newman, T. Kendelewicz, R. Cao, C. McCants, P. Mahowalk, K. Miyano, and I. Lindau, J. Vac. Sci. Technol. B6, 1245, (1988).
12. N. Newman, W. S. Petro, T. Kendelewicz, S. H. Pan, S. J. Eglash, and W. E. Spicer, J. Appl. Phys. 57, 1247 (1985).
13. D. Coulman, N. Newman, G. Reid, Z. Liliental-Weber, E. R. Weber, and W. E. Spicer, J. Vac. Sci. Technol. A5, 1521 (1987).
14. Z. Liliental-Weber, J. Washburn, N. Newman, W. E. Spicer, and E. R. Weber, Appl. Phys. Lett. 49, 1514 (1986).
15. Z. Liliental, R. W. Carpenter, and J. Escher, Ultramicroscopy 14, 135 (1984).
16. T. S. Kuan, P. E. Batson, T. N. Jackson, H. Ruppreicht, and E. L. Wilkie, J. Appl. Phys. 54, 6952 (1983).
17. T. Yoshiie, C. L. Bauer, and A. G. Milnes, Thin Solid Films 111, 149 (1984).
18. A. Miret, N.Newman, E. R. Weber, Z. Liliental-Weber, J. Washburn, and W. E. Spicer, J. Appl. Phys. 63, 2006 (1988).
19. N. Newman, Z. Liliental-Weber, E. R. Weber, J. Washburn, and W. E. Spicer, Appl. Phys. Lett. 53, 145 (1988).
20. Z. Liliental-Weber, A. Miret-Goutier, N. Newman, C. Jou, W. E. Spicer, J. Washburn, and E. R. Weber, Mat. Res. Soc. Symp. Proc. 102, 241 (1988).
21. C. J. Jou, J. Washburn, Z. Liliental-Weber, and R. Gronsky, J. Electrochem. Soc. (1988) (in press).
22. W. E. Spicer, N. Newman, T. Kendelewicz, W. G. Potro, M. D. Williams, C. E. McCants, and I. Lindau, J. Vac. Sci. Technol. B3, 1178 (1985).
23. R. Ludeke and G. Landgreen, J. Vac. Sci. Technol. 19, 667 (1981).

24. Z. Liliental-Weber, C. Nelson, R. Gronsky, J. Washburn, and R. Ludeke, Mat. Res. Soc. Symp. Proc. 77, 229 (1987).
25. N. Newman, W. E. Spicer, and R. R. Weber, J. Vac. Sci. Technol. B5, 1020 (1987).
26. S. P. Svensson, G. Landgreen and T. G. Andersson, J. Appl. Phys. 54, 4475 (1983).
27. N. Newman, K. K. Chin, W. G. Petro, T. Kendelewski, M. D. Williams, C. E. McCants and W. E. Spicer, J. Vac. Sci. Technol. A3, 996 (1985).
28. N. Newman, W. E. Spicer and E. R. Weber, J. Vac. Sci. Technol. B5, 1020 (1987).
29. Z. Liliental, N. Newman, J. Washburn, and E. R. Weber, Appl. Phys. Lett. (1988) (in press).
30. A. B. McLean and R. H. Williams, J. Phys. C. Sol. State. Phys. 21, 783 (1988).
31. J. R. Waldrop, J. Vac. Sci. Technol. B2, 445 (1986).
32. T. Yoshiie and C. L. Bauer, J. Vac. Sci. Technol. A1, 554 (1983).
33. T. T. Sands, J. Washburn, and R. Gronsky, Mater. Lett. 3, 247 (1985).
34. O. R. Monteiro and J. W. Evans, J. Vac. Sci. Technol. (1989) (in press).

LAWRENCE BERKELEY LABORATORY
CENTER FOR ADVANCED MATERIALS
1 CYCLOTRON ROAD
BERKELEY, CALIFORNIA 94720